

Decoding the message from meteoritic stardust silicon carbide grains

Karen M. Lewis

Monash Centre for Astrophysics (MoCA), Monash University, Clayton VIC 3800, Australia

Earth and Planetary Sciences, Tokyo Institute of Technology, Japan

karen.michelle.lewis@gmail.com

Maria Lugaro

Monash Centre for Astrophysics (MoCA), Monash University, Clayton VIC 3800, Australia

maria.lugaro@monash.edu

Brad K. Gibson and Kate Pilkington

Jeremiah Horrocks Institute, University of Central Lancashire, UK

Monash Centre for Astrophysics (MoCA), Monash University, Clayton VIC 3800, Australia

bkgibson@uclan.ac.uk, kpilkington@uclan.ac.uk

ABSTRACT

Micron-sized stardust grains that originated in ancient stars are recovered from meteorites and analysed using high-resolution mass spectrometry. The most widely studied type of stardust is silicon carbide (SiC). Thousands of these grains have been analysed with high precision for their Si isotopic composition. Here we show that the distribution of the Si isotopic composition of the vast majority of stardust SiC grains carry the imprints of a spread in the age-metallicity distribution of their parent stars and of a power-law increase of the relative formation efficiency of SiC dust with the metallicity. This result offers a solution for the long-standing problem of silicon in stardust SiC grains, confirms the necessity of coupling chemistry and dynamics in simulations of the chemical evolution of our Galaxy, and constrains the modelling of dust condensation in stellar winds as function of the metallicity.

Subject headings: dust, extinction — meteorites, meteors, meteoroids — Galaxy: abundances — stars: AGB and post-AGB

1. Introduction

A small fraction (order of 1-100 parts per million in mass) of the matrix of primitive meteorites is composed of *stardust* grains. These grains originated in stars, were present at the formation of the Solar System, and have been preserved inside meteorites in their original form until today. Since their discovery in the late 1980s stardust grains have been extensively analysed and employed to constrain our understanding of nucleosynthesis, mixing, and dust formation in stars and supernovae, Galactic chemical evolution (GCE), processing of dust in the interstellar medium, the formation of the Solar System, and the evolution of meteorite parent bodies (Bernatowicz & Zinner 1997; Clayton & Nittler 2004). A large variety of minerals have been discovered as stardust, from diamond, to silicate and Al_2O_3 grains. Among them, silicon carbide (SiC) grains have been the most widely studied both due to their relatively large size (up to several μm), as compared to other types of stardust, and to the relatively easier separation procedure. The vast majority of the stardust SiC grains recovered from meteorites show the clear signature of an origin in the mass-losing envelopes of asymptotic giant branch (AGB) stars (Gallino et al. 1990; Lugaro et al. 2003) that become C rich ($\text{C} > \text{O}$) due to dredge-up of material from the deep C-rich layers into the convective envelope of the star. In C-rich conditions some C is free from the strong CO molecular bond and can react with Si to form SiC. Stardust SiC grains of C-rich AGB origin are the “mainstream” population, which comprises $>93\%$ of all stardust SiC, and the minor Y and Z populations, which comprise $\simeq 1\%$ each of all stardust SiC. The Si compositions of mainstream, Y, and Z grains carry the signature of both the initial composition of their parent star, which is determined by GCE, and the neutron-capture and mixing processes that occurred in the AGB parent stars (Zinner et al. 2006). The typical Si isotopic ratios of the Y and Z grains point to AGB parent stars of average metallicity $\simeq 1/2$ and $\simeq 1/3$, respectively, of solar, while the Si isotopic ratios of mainstream grains suggest a close-to-solar metallicity for their parent stars (Hoppe et al. 1997; Amari et al. 2001; Zinner et al. 2006).

A large amount of high-precision Si isotope data from stardust SiC has been collected in the past 25 years (Figure 1), however, their distribution is not understood. A particularly irksome problem is that most mainstream grains have $^{29}\text{Si}/^{28}\text{Si}$ and $^{30}\text{Si}/^{28}\text{Si}$ larger than solar (up to $+20\%$) while according to GCE models the $^{29}\text{Si}/^{28}\text{Si}$ and $^{30}\text{Si}/^{28}\text{Si}$ ratios increase with metallicity, which in turn increases with time (Timmes & Clayton 1996). The grains must have formed in stars of metallicity higher than solar, however, their parent stars must have died before the Solar System formed. Several possible explanations have been proposed for this apparent paradox, from a simple model of stellar migration from the inner part of the Galaxy (Clayton 1997), which has difficulties in reproducing the observed distribution (Nittler & Alexander 1999), to inhomogeneities in the interstellar medium (Lugaro et al. 1999), which is at odds with the correlation between the Si and Ti isotopic composition of

the grains (Nittler 2005), to a starburst triggered by the merging of our Galaxy with another galaxy (Clayton 2003). To address this problem, we use the measured $\delta^{29}\text{Si}$ and $\delta^{30}\text{Si}$ of SiC grains from AGB stars (Figure 1) to derive the age-metallicity relation (AMR) of their parent stars and compare it to that observed for stars in the solar neighbourhood.

2. Method

We selected from the Presolar Grain Database (Hynes & Gyngard 2009) the 2,732 main-stream, 133 Y, and 92 Z grains with 1σ error bar lower than 15‰. For each grain we applied the following steps:

1. We inferred the metallicity $[\text{Fe}/\text{H}]$ (defined as the logarithm of the Fe/H ratio with respect to solar) of the parent star of each SiC grain from the relationship between $\delta^{29}\text{Si}$ and $[\text{Fe}/\text{H}]$ predicted by different GCE models (Figure 2). All the models have been renormalised so that at the time of the formation of the Sun, set to 8.5 Gyr, $[\text{Fe}/\text{H}]=0$ and $\delta^{29}\text{Si}=0$, by definition. Before normalisation, all the models produce $\delta^{29}\text{Si}$ between -600 and -400 at $[\text{Fe}/\text{H}]=0$, a long-standing problem probably related to the rates of the nuclear reactions that produce ^{29}Si in core-collapse supernovae (Hoppe et al. 2009).
2. We estimated the change in $\delta^{30}\text{Si}$ resulting from AGB nucleosynthesis as the distance $\Delta^{30}\text{Si}$ between the measured $\delta^{30}\text{Si}$ and the value obtained from the GCE line. We assumed that the best fit to the Si isotopic ratios in the Si three-isotope plot (the “mainstream line”) shifted by -15 in $\delta^{30}\text{Si}$ represents the GCE of the Si isotopic ratios (Figure 1). This shift is in agreement with the Si composition of stardust silicate grains from AGB stars, which represents the Si composition of O-rich AGB stars as unaltered by nucleosynthesis and dredge-up (Mostefaoui & Hoppe 2004; Nguyen et al. 2010).
3. We derived the parent star age from its mass as obtained from $\Delta^{30}\text{Si}$ using the set of FRANEC C-rich AGB models with the neutron-capture cross sections of the Si isotopes by Guber et al. (2003) presented in Zinner et al. (2006), to which we added the age of the Sun. In these models the mass-loss rate was included using the parametrization given by Reimers (1975). For the $1.5 M_{\odot}$ and $2 M_{\odot}$ models results were presented for different values of the associated free parameter $\eta=0.1, 0.3, 0.5$ and we choose to average the results for each mass. A range of $\Delta^{30}\text{Si}$ is allowed during the C-rich phase of each model since $\Delta^{30}\text{Si}$ increases with the number of dredge-up episodes. This results in different possible masses associated to the same $\Delta^{30}\text{Si}$, in particular when its value is small. We chose to remove this degeneracy by taking as the best representative of

each model the Si composition reported after the last computed dredge-up episode. Most SiC grains formed with the composition present in the envelope after the final few dredge-ups since the largest fraction of the envelope mass during the C-rich phase is lost in these final phases. For example, considering the $3 M_{\odot}$ model with $Z = 0.02$, more than 2/3 of the envelope mass during the C-rich phase is lost after the third-last TDU episode, and roughly 1/2 is lost after the very last TDU episode (see Table 4 of Straniero et al. 1997). Note that we did not include in our age determination the up to 1 Gyr of grain residence time in the interstellar medium (Gyngard et al. 2009).

4. Since also $\delta^{29}\text{Si}$ can be marginally affected by AGB nucleosynthesis we improved the estimates of age and metallicity by repeating the same procedure as above with a new initial $\delta^{29}\text{Si}_{\text{new}} = \delta^{29}\text{Si} - \Delta^{29}\text{Si}$, with $\Delta^{29}\text{Si}$ derived from the same AGB model predictions used to match $\Delta^{30}\text{Si}$.

3. Results and discussion

The resulting SiC AMR is plotted in Figure 3 together with the AMR derived for stars in the solar neighbourhood from the Geneva-Copenhagen (G-C) survey (Holmberg et al. 2007).

The SiC ages are affected by several uncertainties. First, there are random uncertainties related to the measurement errors. We made the conservative choice to plot the lower limits of the ages derived from adding the experimental 2σ error bar to $\delta^{30}\text{Si}$. Second, there are random errors related to the possible effect of inhomogeneities in the interstellar medium, which may change the Si composition of any given parent stars by $\sim 50\%$ (Lugaro et al. 1999; Nittler 2005). These are not possible to be evaluated. Assuming that the silicon isotopic distribution is relatively symmetric, the age and the metallicity calculated for grains at the peak of the distribution should be reliable. Third, there are systematic uncertainties related to the choice of the line taken to represent the GCE in the Si isotope plot (Figure 1) and to the AGB model predictions. The uncertainty related to the GCE line would most likely result in smaller stellar ages as the line could be shifted further away from the mainstream line than what we have assumed and still be in agreement with the silicate data. Instead, it is not known if the uncertainty related to the AGB models would result in smaller or larger stellar ages since both larger and smaller $\Delta^{30}\text{Si}$ for a given stellar mass are possible within the uncertainties wrought by, e.g., the mass-loss rate, the efficiency of the dredge-up of the deep layers of the stars into the convective envelope, and the neutron-capture cross section of the Si isotopes.

Nonwithstanding the uncertainties discussed above, relatively, the ages derived for the

parent stars of the Y grains are similar to those of the mainstream grains, while those derived for the Z grains cover a much narrower range indicating that Z grains have on average parent stars of higher mass than mainstream and Y grains. This result supports proton captures at the base of the convective envelope (also known as “hot bottom burning”) as the process responsible for lowering the $^{12}\text{C}/^{13}\text{C}$ ratios in the Z grains (ranging from 20 to 100) with respect to those observed in the Y grains (> 100 , by definition). If this interpretation is correct, GCE models are not required to match the $\delta^{29}\text{Si}$ versus $[\text{Fe}/\text{H}]$ relationship of Zinner et al. (2006) (Figure 2), which was derived using AGB models of fixed mass lower than $\sim 3 M_{\odot}$. On the other hand, one may wonder why there are no SiC grains from low-metallicity and low-mass parent stars. A possibility is that the very high C/O ratio reached in these stars (up to 20 - 30) may favour production of amorphous carbon dust rather than SiC (Sloan et al. 2008).

The SiC $[\text{Fe}/\text{H}]$ distribution is determined by the steepness of the $\delta^{29}\text{Si}$ versus $[\text{Fe}/\text{H}]$ relationship, which varies with the choice of the core-collapse supernova (SNII) yields and the GCE model (Figure 2). The *GEtool* (Fenner & Gibson 2003) chemical evolution model was computed with dual infall (i.e., a rapid formation of the halo, followed by subsequent, protracted, disk formation), initial mass function from Kroupa et al. (1993), and a Schmidt-Kennicutt star formation prescription, and it is tuned to recover the gas and stellar abundances and radial surface densities in the Milky Way. In Figure 3 we plot two SiC AMRs obtained using the most and the least steep $\delta^{29}\text{Si}$ versus $[\text{Fe}/\text{H}]$ relationships from the *GEtool* simulations. These corresponds to using the yields by Woosley & Weaver (1995) and Kobayashi et al. (2006), respectively. The *GEtool* model computed using the SNII yields from Kobayashi et al. (2006) and that computed using Chieffi & Limongi (2004) produce a very similar SiC AMR with a $[\text{Fe}/\text{H}]$ spread of a factor of three, within that observed in the G-C survey. Timmes & Clayton (1996) and Kobayashi et al. (2011) obtained a much steeper and much flatter, respectively, $\delta^{29}\text{Si}$ and $[\text{Fe}/\text{H}]$ relationship than the *GEtool* models presented here. The difference depends on many of the ingredients of the GCE simulation, e.g., the initial mass function and the infall scheme, which also affect the theoretical AMR predicted directly by the GCE models. Interestingly, GCE models that predict a steeper $\delta^{29}\text{Si}$ versus $[\text{Fe}/\text{H}]$ relationship also predict a flatter AMR. As a consistency check, in the right panel of Figure 3 the AMRs predicted by the different GCE models considered here are compared to the G-C stars. None of the models can recover the observed AMR. A better match may be found by recent models that consider dynamics together with the chemical evolution in the Galaxy (Kobayashi & Nakasato 2011; Pilkington et al. 2012). However, we do not consider them here as they have not been extended yet to include the evolution of isotopic abundances. *Overall, the SiC grain data confirm the result of the G-C survey that stars exist with ages older than the Sun and metallicities higher than the Sun.*

To make a quantitative comparison of the metallicity distribution function (MDF) derived for the SiC grain parent stars and for the G-C stars we restrict ourselves to the mainstream SiC grains as they represent the least biased sample. We removed the Y and Z grains because their numbers are probably overestimated due to specific searches dedicated to identifying these types of grains. In the left panel of Figure 4 we compare the MDF obtained from the SiC AMR to that obtained from the G-C survey. Because the 1σ error bar on the grain $[\text{Fe}/\text{H}]$ that derives from the experimental uncertainty of $\delta^{29}\text{Si}$ is much smaller (<0.03 dex) than that of the stellar $[\text{Fe}/\text{H}]$ (~ 0.1 dex), for better comparison we convolved the grain $[\text{Fe}/\text{H}]$ data with a Gaussian of $\sigma=0.1$. The main difference between the grain and the stellar MDF is that the mean metallicity of the parent stars of the mainstream SiC grains is $\simeq 50\%$ higher than that of the G-C stars. We interpret this as a selection effect between the grain and the star samples indicating that formation of SiC dust is favored by higher metallicity. We define the SiC relative formation efficiency (RFE) as the ratio between the normalised number of mainstream SiC grains and of G-C stars in each metallicity bin and plot these values in the right panel of Figure 4. The SiC RFE is unitless and its values are not absolute, but have a meaning only when considered relatively to each other. We infer that the SiC RFE can be represented by a power law in metallicity. The relationship is well defined only for values of $[\text{Fe}/\text{H}]$ between ± 0.3 dex because in this range there are sufficient numbers of both mainstream SiC grains and G-C stars to make their ratio statistically meaningful.

An important systematic uncertainty in the derivation of the SiC RFE is related to the renormalised value of $\delta^{29}\text{Si}=0$ at $[\text{Fe}/\text{H}]=0$ (Item 1 of Sec. 2) Such renormalisation may easily be a few percent wrong, in particular due to the effect of inhomogeneities in the interstellar medium, which produce variations in $\delta^{29}\text{Si}$ of the order of 70‰ for the same $[\text{Fe}/\text{H}]$ within ± 0.01 (Nittler 2005). If $\delta^{29}\text{Si}$ is renormalised to a positive value instead of zero, clearly the grain MDF becomes closer to that of the G-C survey and the derived SiC RFE is less steep. In Figure 4 we also present the results obtained by setting $\delta^{29}\text{Si}=50\%$ at $[\text{Fe}/\text{H}]=0$. The SiC RFE still increases with the metallicity, though the increase is less pronounced and disappears between $0 < [\text{Fe}/\text{H}] < 0.1$. We consider this example as an upper limit: a choice of $\delta^{29}\text{Si} \sim 30\%$ at $[\text{Fe}/\text{H}]=0$ is probably more realistic being the value shown by the largest number of SiC, according to Figure 13 of Nittler & Alexander (2003).

4. Conclusions

The results presented here confirm that the relationship between age and metallicity in the Galaxy is relatively flat and that a spread of metallicities is present for each age. This cannot be recovered by traditional GCE models and requires a more sophisticated approach in-

cluding coupling of Galactic dynamics and chemical evolution (Kobayashi & Nakasato 2011; Pilkington et al. 2012). Scattering and radial migration must have played an important role in determining the properties of stars in the solar neighbourhood (Clayton 1997), as supported by recent observational studies (e.g. Boeche et al. 2013; Ramírez et al. 2013).

We have interpreted the shift of the SiC MDF to higher metallicities than the G-C survey as a selection effect and derived that the SiC relative formation efficiency increases with the stellar metallicity as a power law. This result is in qualitative agreement with Spitzer observations of C-rich AGB stars in the Large and Small Magellanic Clouds (Sloan et al. 2008), which indicate that the mid-infrared emission from SiC and silicate dust decreases with the metallicity, while the emission from amorphous carbon dust does not. On the basis of this evidence, we tentatively predict that the MDF of stardust silicates (Mostefaoui & Hoppe 2004; Nguyen et al. 2010) should be similar to that of SiC grains, while the MDF of stardust graphite grains from C-rich AGB stars (Jadhav et al. 2008) should be similar to that of the G-C survey. Nittler (2009) conducted a similar exercise to ours based on the O ratios in stardust oxide grains and found evidence for the existence of a moderate AMR. If the $^{18}\text{O}/^{16}\text{O}$ ratio is a good indicator of the stellar metallicity, we expect a correlation between $^{18}\text{O}/^{16}\text{O}$ and $\delta^{29}\text{Si}$, which is not shown by the stardust silicate grains, but could be masked by the effect of dilution with normal material (Nguyen et al. 2010). It should also be noted that stardust oxide and silicate grains are more likely to come from lower-mass stars than SiC grains (Gail et al. 2009), which may result in a different AMR. It will be possible to statistically investigate these issues in the future when more high-precision Si data for these types of stardust are available.

The first two authors have equally contributed to this paper. We thank Chiaki Kobayashi and Mike Savina for discussion and Keith Hsuan for technical support. We thank the anonymous referee for helping us to greatly improve the treatment and discussion of the uncertainties. ML is an ARC Future Fellow and Monash Fellow. This project was supported by the Monash University “Advancing Women in Research” grant.

REFERENCES

- Amari, S., Nittler, L. R., Zinner, E., Gallino, R., Lugaro, M., & Lewis, R. S. 2001, *ApJ*, 546, 248
- Bernatowicz, T. J. & Zinner, E., eds. 1997, *American Institute of Physics Conference Series*, Vol. 402, *Astrophysical implications of the laboratory study of presolar materials*

- Boeche, C. et al. 2013, A&A, accepted (astro-ph: 1302.3466)
- Chieffi, A. & Limongi, M. 2004, ApJ, 608, 405
- Clayton, D. D. 1997, ApJ, 484, L67
- . 2003, ApJ, 598, 313
- Clayton, D. D. & Nittler, L. R. 2004, ARA&A, 42, 39
- Fenner, Y. & Gibson, B. K. 2003, PASA, 20, 189
- Gail, H.-P., Zhukovska, S. V., Hoppe, P. & Trieloff, M. 2009, ApJ, 698, 1136
- Gallino, R., Busso, M., Picchio, G., & Raiteri, C. M. 1990, Nature, 348, 298
- Groenewegen, M. A. T., van den Hoek, L. B. & de Jong, T. 1995, A&A, 293, 381
- Guber, K. H., Koehler, P. E., Derrien, H., Valentine, T. E., Leal, L. C., Sayer, R. O., & Rauscher, T. 2003, Phys. Rev. C, 67, 062802
- Gyngard, F., Amari, S., Zinner, E., & Ott, U. 2009, ApJ, 694, 359
- Holmberg, J., Nordström, B., & Andersen, J. 2007, A&A, 475, 519
- Hoppe, P., Annen, P., Strebel, R., Eberhardt, P., Gallino, R., Lugaro, M., Amari, S., & Lewis, R. S. 1997, ApJ, 487, L101
- Hoppe, P., Leitner, J., Meyer, B. S., The, L.-S., Lugaro, M., & Amari, S. 2009, ApJ, 691, L20
- Hynes, K. M. & Gyngard, F. 2009, in Lunar and Planetary Inst. Technical Report, Vol. 40, Lunar and Planetary Institute Science Conference Abstracts, 1198
- Jadhav, M., Amari, S., Marhas, K. K., Zinner, E., Maruoka, T., & Gallino, R. 2008, ApJ, 682, 1479
- Kobayashi, C., Karakas, A. I., & Umeda, H. 2011, MNRAS, 414, 3231
- Kobayashi, C. & Nakasato, N. 2011, ApJ, 729, 16
- Kobayashi, C., Umeda, H., Nomoto, K., Tominaga, N., & Ohkubo, T. 2006, ApJ, 653, 1145
- Kroupa, P., Tout, C. A., & Gilmore, G. 1993, MNRAS, 262, 545

- Lugaro, M., Davis, A. M., Gallino, R., Pellin, M. J., Straniero, O., & Käppeler, F. 2003, *ApJ*, 593, 486
- Lugaro, M., Zinner, E., Gallino, R., & Amari, S. 1999, *ApJ*, 527, 369
- Mostefaoui, S. & Hoppe, P. 2004, *ApJ*, 613, L149
- Nguyen, A. N., Nittler, L. R., Stadermann, F. J., Stroud, R. M., & Alexander, C. M. O. 2010, *ApJ*, 719, 166
- Nittler, L. R. 2005, *ApJ*, 618, 281
- Nittler, L. R. 2009, *PASA*, 26, 2871
- Nittler, L. R. & Alexander, C. M. O. 1999, *ApJ*, 526, 249
- Nittler, L. R. & Alexander, C. M. O. 2003, *Geochim. Cosmochim. Acta*, 67, 4961
- Pilkington, K., Gibson, B. K., Brook, C. B., Calura, F., Stinson, G. S., Thacker, R. J., Michel-Dansac, L., Bailin, J., Couchman, H. M. P., Wadsley, J., Quinn, T. R., & Maccio, A. 2012, *MNRAS*, 425, 969
- Ramírez, I., Allende Prieto, C., & Lambert, D. L. 2013, *ApJ*, 764, 78
- Reimers, D. 1975, in *Problems in stellar atmospheres and envelopes*, ed. Baschek, B., Kegel, W. H., & Traving, G., 229
- Sloan, G. C., Kraemer, K. E., Wood, P. R., Zijlstra, A. A., Bernard-Salas, J., Devost, D., & Houck, J. R. 2008, *ApJ*, 686, 1056
- Straniero, O., Chieffi, A., Limongi, M., Busso, M., Gallino, R., & Arlandini, C. 1997, *ApJ*, 478, 332
- Timmes, F. X. & Clayton, D. D. 1996, *ApJ*, 472, 723
- Woosley, S. E. & Weaver, T. A. 1995, *ApJS*, 101, 181
- Zinner, E., Nittler, L. R., Gallino, R., Karakas, A. I., Lugaro, M., Straniero, O., & Lattanzio, J. C. 2006, *ApJ*, 650, 350

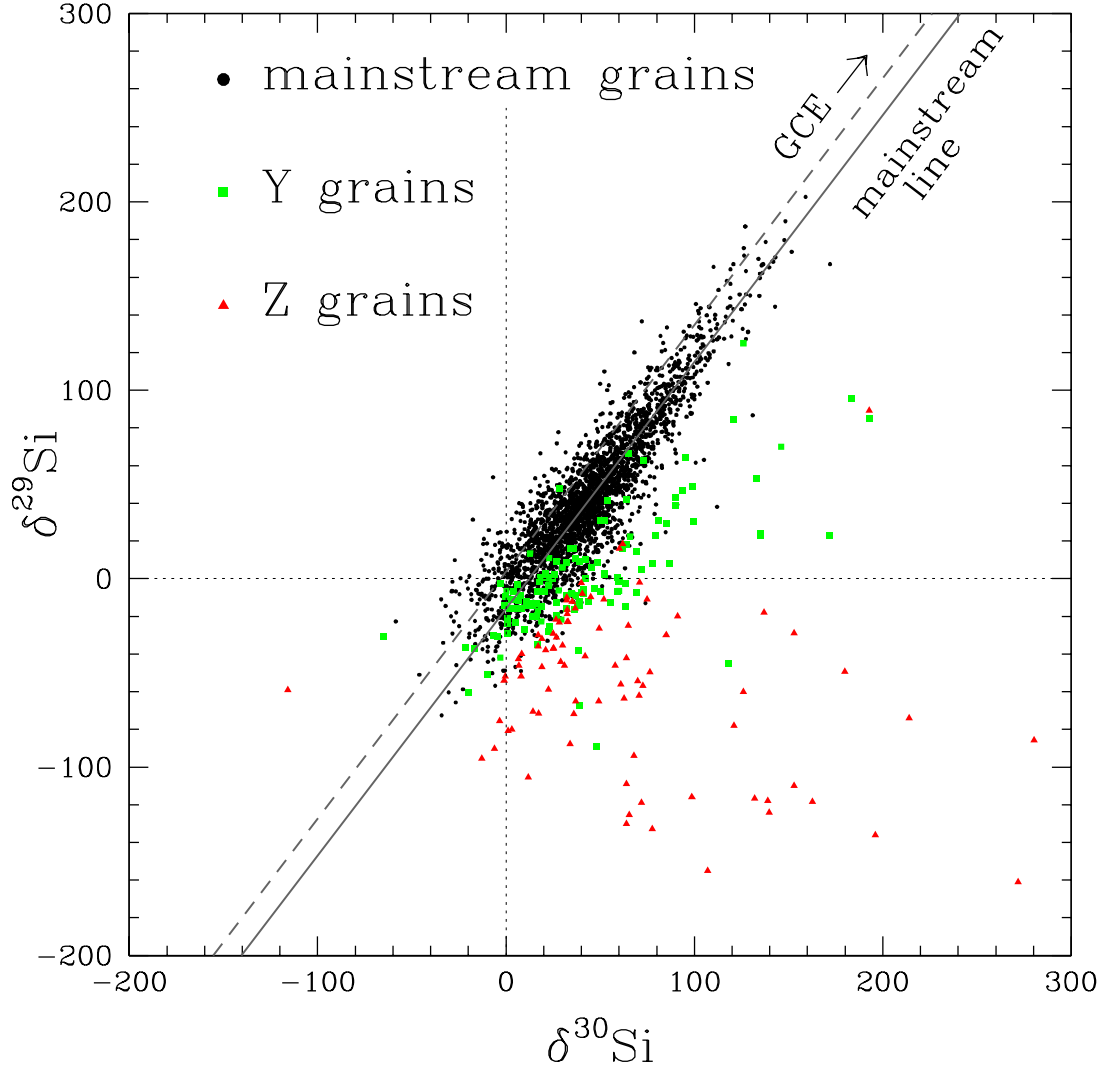


Fig. 1.— Distribution of the Si isotopic compositions of SiC mainstream, Y, and Z grains with 1σ error bar lower than 15‰ represented using the $\delta^{29,30}\text{Si}$ notation, i.e., the permil variation of $^{29,30}\text{Si}/^{28}\text{Si}$ with respect to the solar ratios. The solid line is the best fit through the mainstream SiC data (“mainstream line”) of slope 1.31 and intercept -15.9‰ . The dashed line is the mainstream line shifted by -15‰ in $\delta^{30}\text{Si}$. This is taken to represent the GCE of the Si isotopic ratios, with $\delta^{29,30}\text{Si}$ increasing with the metallicity.

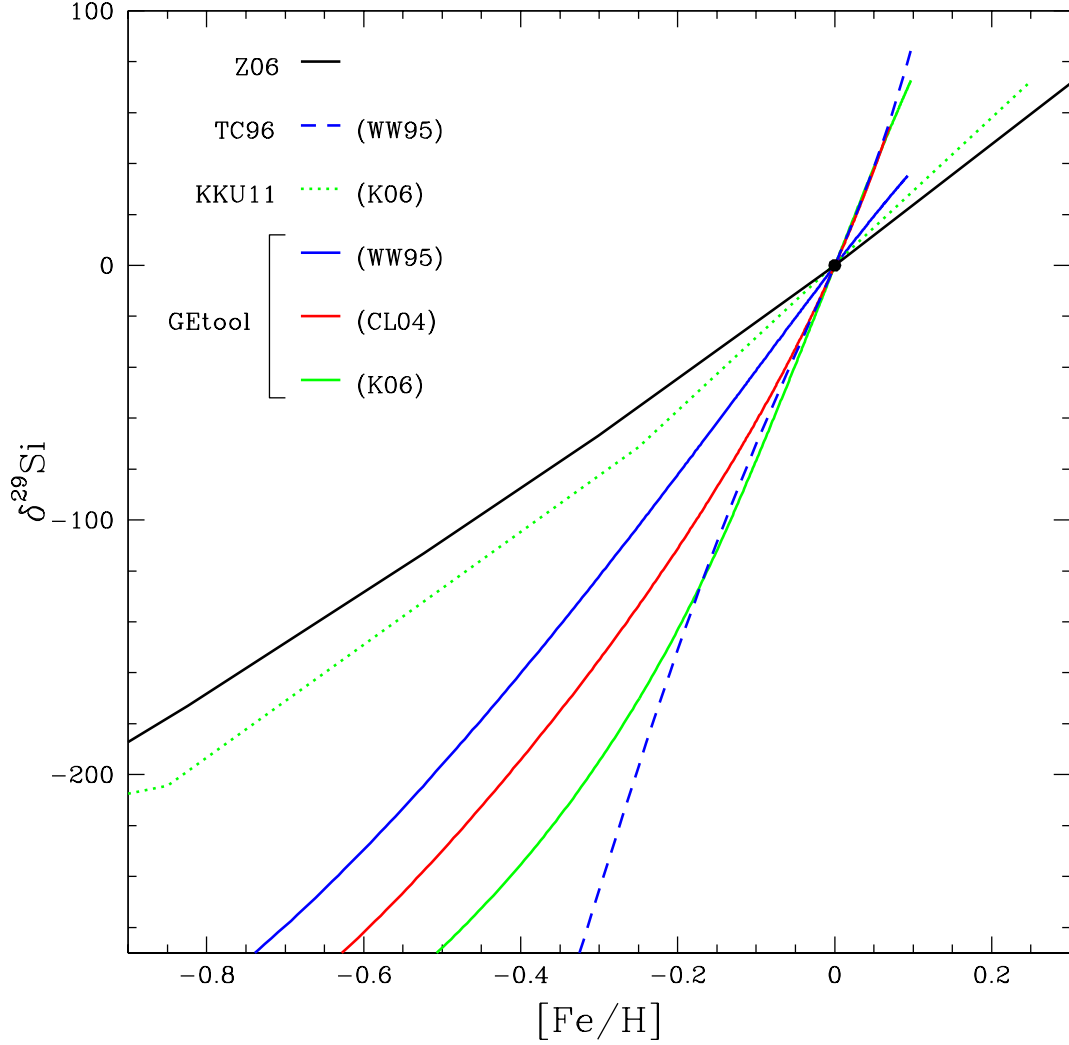


Fig. 2.— The relationship between $\delta^{29}\text{Si}$ and $[\text{Fe}/\text{H}]$ derived from different GCE models: TC96 (Timmes & Clayton 1996), K06 (Kobayashi et al. 2011), and GTool (Fenner & Gibson 2003), using different SNII yields: WW95 (Woosley & Weaver 1995), CL04 (Chieffi & Limongi 2004), and K06 (Kobayashi et al. 2006); or by simply assuming that the abundances of ^{29}Si and ^{30}Si scale with the metallicity, while that of ^{28}Si is α enhanced such that ^{28}Si is 1/8 of its solar abundance when the metallicity is 1/10 of solar: Z06 (Zinner et al. 2006). This choice produces a $\delta^{29}\text{Si}$ and $[\text{Fe}/\text{H}]$ relationship close to that obtained by Zinner et al. (2006) comparing the composition of Z grains to AGB models of fixed mass and variable metallicity.

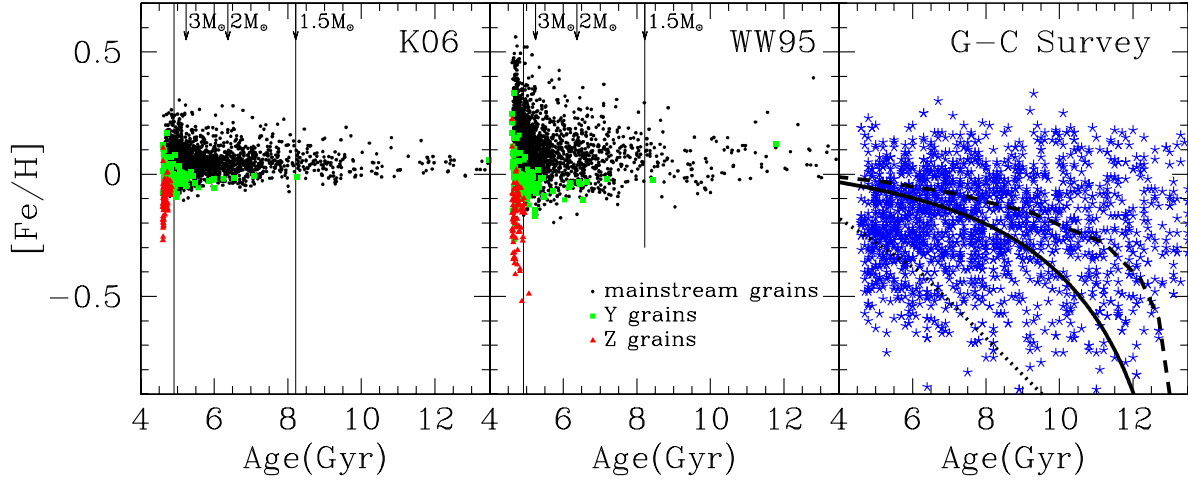


Fig. 3.— The age-metallicity relation (AMR) derived for the parent stars of SiC mainstream, Y, and Z grains using GETool with two different sets of SNII yields: K06 (Kobayashi et al. 2006, left panel) and WW95 (Woosley & Weaver 1995, middle panel). Note that the plotted ages are lower limits based on the experimental 2σ error bar. The upper limits are undetermined (because of negative $\Delta^{30}\text{Si}$) and >13 Gyr for 54% and 26% of the mainstream grains, respectively, while they are <6 Gyr for 86% of the Z grains. Selected initial stellar masses are indicated at the top of the panels in correspondance to their ages. Note that only AGB stars in the mass range between $\sim 1.5 M_{\odot}$ and $\sim 4 M_{\odot}$ are expected to become C rich and produce SiC grains (Groenewegen et al. 1995; Gail et al. 2009). The corresponding age limits are highlighted by the two vertical thin black lines, however, we did not remove the points outside this range because (i) they are lower limits and (ii) they could shift inside the allowed range when considering the several uncertainties discussed in the text. The right panel shows the AMR obtained from the Geneva-Copenhagen (G-C) survey for 2037 stars in the solar neighbourhood with age uncertainties lower than 25%, as compared to the AMRs predicted by the different GCE models: GETool (solid line, which is independent of the choice of the yields); TC96 (dashed line, Timmes & Clayton 1996); KKU11 (dotted line, Kobayashi et al. 2011).

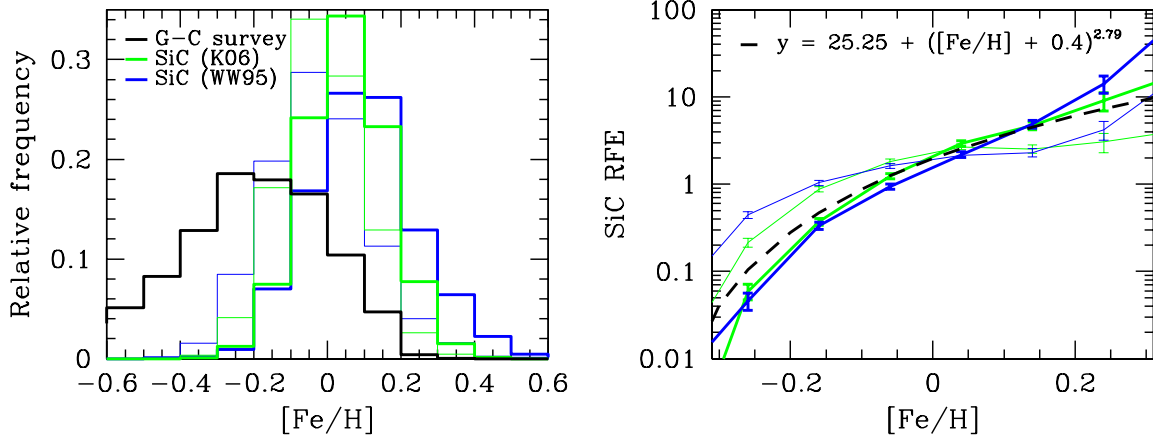


Fig. 4.— The metallicity distribution function (MDF) of the parent stars of mainstream SiC grains derived using GEttool and two different sets of SNII yields: WW95 (Woosley & Weaver 1995) and K06 (Kobayashi et al. 2006), is compared to that obtained for stars in the solar neighbourhood from the Geneva-Copenhagen (G-C) survey (left panel). The SiC relative formation efficiency (RFE) of as function of the $[\text{Fe}/\text{H}]$ is shown in the right panel. The thin lines present the results obtained renormalising $\delta^{29}\text{Si}=50\%$ at $[\text{Fe}/\text{H}]=0$ and the black dashed line is a proposed power-law fit.